On the origin of mascon basins on the Moon (and beyond)

Andrew J. Dombard,[1] Steven A. Hauck, II,[2] and Jeffrey A. Balcerski[2]

Received 19 October 2012; revised 29 November 2012; accepted 29 November 2012; published 15 January 2013.

[1] Mascon basins on the Moon are large craters that display significant positive free-air and Bouguer gravity anomalies. An important question is why is not every large crater a mascon, as less than half have been previously determined to be. We detrend the free-air, topographic, and Bouguer gravity anomalies and find that most large basins (28 of 41) display mascon characteristics (e.g., strong positive Bouguer anomalies narrower than the surface rims). Negative free-air gravity annuli surrounding the central highs generally are absent in the Bouguer gravity, implicating surface topography. We propose that beneath a forming large basin, the relatively narrow transient crater drives mantle uplift, while upward *and* inward collapse forms the surface topography. Furthermore, the nonmascon basins are all ancient and heavily degraded, indicating a postimpact evolutionary process. Our results suggest that mascon formation is the standard for large impacts on the Moon and by extension on other terrestrial planets. **Citation:** Dombard, A. J., S. A. Hauck, II, and J. A. Balcerski (2013), On the origin of mascon basins on the Moon (and beyond), *Geophys. Res. Lett.*, *40*, 28–32, doi:10.1029/2012GL054310.

1. Introduction

[2] Large impact craters provide a window into the crustal structure of terrestrial planets. For the Moon however, that window has been a little foggy. Since the days of Apollo [*Müller and Sjogren*, 1968], it has been known that many large impact basins possess a centrally located, positive free-air gravity anomaly (the *mascon* basins), in perplexing contrast to the negative anomaly that should arise from what is, in essence, a big hole in the ground. Although the origin of the excess gravity from these and subsequently discovered basins has been debated [e.g., *Wise and Yates*, 1970; *Phillips et al*., 1972; *Neumann et al*., 1996; *Wieczorek and Phillips*, 1999], the fact remains that these mascon basins are the scars left by large impacts on a volcanically active terrestrial world. Thus, one might expect that all large craters on the Moon (and the other terrestrial planets for that matter) with characteristics of a mascon basin should be common and perhaps pervasive. A catalog of mascon basins from the first truly global gravity models of the Moon derived from the Japanese Kaguya (SELENE) mission [*Namiki et al*., 2009], however, indicated less than half of the largest craters are mascons. A previous assessment by *Mohit and Phillips* [2006], which argued that nonmascon basins (and the mare-filled mascons seen in the Apollo era) evolved from mascons, was hampered by low-resolution, high-error gravity on the far-side, where tracking of a spacecraft from Earth is precluded, and thus did not consider all large craters on the Moon.

[3] In light of the imminent release of the global, high-resolution gravity data from NASA's Gravity Recovery and Interior Laboratory (GRAIL) mission [*Zuber et al*., 2012], we reexamine all large craters on the Moon, finding that most display the characteristics of a mascon basin. We utilize the results of this analysis to address the fundamental question of why all large craters on terrestrial planets are not mascon basins.

2. Craters and Their Gravities

[4] We examine all 41 craters 300 km in diameter or greater (see Table S1 in the Supporting Information), a subset of all lunar craters as compiled by the Lunar and Planetary Institute (http://www.lpi.usra.edu/lunar/surface/Lunar_Impact_Crater_Database_v24May2011.xls), noting the basins' diameter, location, and age. We omit South Pole-Aitken Basin, because we consider it in a class by itself. Mascons are primarily identified by their gravity signatures. Thus, we use the most recent gravity model (SGM100i) derived from global data from the Japanese Kaguya mission (http://l2db.selene.darts.isas.jaxa.jp/index.html.en), which is a spherical harmonic model of the potential complete to degree and order 100 (full-wavelength resolution of ~110 km) with the ratio of the power spectra of the coefficients and the uncertainties less than ~2 only for degrees above 80. GRAIL data will refine, though not supersede, the gravity model at the dominant length scales of these largest craters. Knowledge of the component of the observed gravity arising from surface topography is critical to exploring the gravity from the subsurface; thus we use the quarter-degree gridded shape from the Lunar Orbiter Laser Altimeter on the Lunar Reconnaissance Orbiter (http://geo.pds.nasa.gov/missions/lro/lola.htm). We convert this shape into a spherical harmonic model for the component of the gravitational potential due to surface topography using the finite amplitude method of *Wieczorek and Phillips* [1998], assuming a surface density of 2800 kg m^{-3} [cf. *Namiki et al*., 2009]. We have confirmed that the character of the potential field from surface topography does not change if this density differs from this assumption by as much as 200 kg m^{-3}.

[5] We expand out to degree-and-order 100 the potential coefficients into maps of the free-air, topographic, and Bouguer (free-air minus topographic) gravity anomalies. The

All Supporting Information may bbe found in the online version of this article.

[1]Department of Earth and Environmental Sciences, University of Illinois at Chicago, Chicago, Illinois, USA.
[2]Department of Earth, Environmental, and Planetary Sciences, Case Western Reserve University, Cleveland, Ohio, USA.

Corresponding author: A. J. Dombard, Department of Earth and Environmental Sciences, University of Illinois at Chicago, IL, USA. (adombard@uic.edu)

0094-8276/13/2012GL054310

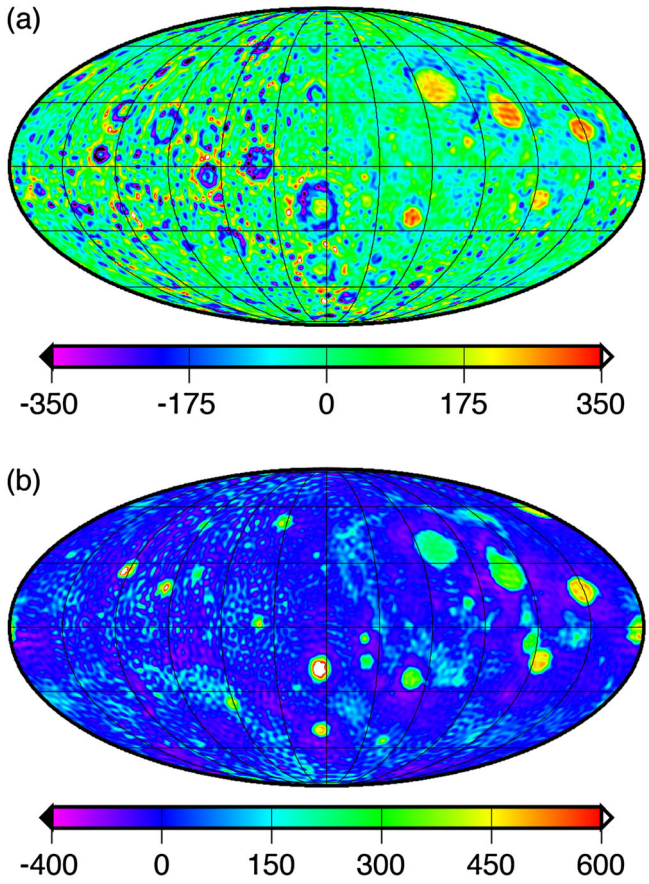

Figure 1. Maps of the free-air (a) and Bouguer (b) gravity anomalies of the Moon, constructed from spherical harmonic expansions from degree 6 through 100. The omission of the first 5 degrees removes long wavelength regional signals, permitting easier analysis of the large basins. The maps are global Mollweide projections centered on 0°N 270°E, with grid lines every 30°. The scale for the Bouguer gravity is piecewise linear between positive and negative values, and the units are mgal.

free-air gravity of the Moon does not display large regional signals; however, the lunar shape (and by extension the Bouguer gravity) does. Large regional signals can mask signals from the smaller basins we consider; thus we detrend the gravity maps by omitting the first 5 spherical harmonic degrees and orders from our expansions. This omitted signal only possesses wavelengths longer than ~2000 km, far wider than the largest crater we consider (Imbrium, 1160 km diameter); detrending the maps in this fashion thus facilitates analysis of the basins by isolating and leveling the background. Maps of the detrended free-air and Bouguer gravity anomalies are shown in Figure 1. Radial profiles of the azimuthally averaged detrended gravity of all candidate craters are shown in Figures S1–S41 (see Supporting Information); averaging around a basin's azimuth also facilitates analysis by smoothing the spectral ringing cause by truncating the expansion at degree 100 (quite apparent as the checkerboard pattern in Figure 1), as well as actual deviations from axisymmetry (e.g., from superposed features like smaller craters). In order to assess the degradation state of the surface morphology of the craters, we cross-reference the gravity anomalies against imagery from the Ultraviolet/Visible Camera on the Clementine Orbiter and topography from Kaguya's Laser Altimeter, as displayed in the Moon function of Google Earth (http://earth.google.com), qualitatively noting whether the feature is readily identifiable as an impact basin (e.g., Al-Khwarizmi-King is not, while Hertzsprung is).

[6] Recent workers have defined suites of mascon types [e.g., *Mohit and Phillips*, 2006; *Namiki et al*., 2009]. Following these recent workers, we define four basin categories. Category A basins are not mascons. They possess a highly degraded surface morphology with a subisostatic (i.e., negative) free-air gravity signature largely reflecting the remaining negative topography of the basin. Category B basins are also generally degraded on the surface, with a fairly broad positive Bouguer gravity signal that balances a negative topographic gravity signal, resulting in a largely isostatic basin. As we will argue below, we consider these basins to be transitional mascons. We classify Category C basins as mascons, with well preserved surface morphologies and the bulls-eye free-air gravity pattern noted by *Mohit and Phillips* [2006] (central high, surrounded by negative then positive annuli). The central free-air gravity high is narrower than the basin rim and is surrounded by a negative gravity annulus also within the rim. Because the central free-air high sits in a gravitational and topographic depression, it may or may not peak at a positive value (both cases are observed). Positive free-air anomalies within topographic depressions reflect a degree of superisostasy, which is a state where there is more mass beneath the surface than would be expected if the topography were isostatically compensated. Category D basins are the mare-dominated mascons, equivalent to Group 2 of *Mohit and Phillips* [2006] and Type PM of *Namiki et al*. [2009]. We assign the craters to each category based on these criteria, although a crater can still be assigned to a type if it deviates in only one criterion (e.g., the Category C Sikorsky-Rittenhouse is fairly degraded on the surface, being overprint by ejecta from Schrödinger).

[7] In contrast to previous analyses, in which fewer than half of the large craters on the Moon were determined to be mascons, we find that most craters 300 km or larger (28 of 41) are mascon basins (see Table S1). Notably, all 13 craters without the gravitational signature of a mascon are also strongly degraded, often nigh impossible to recognize in visible imagery and topography alone. Not surprisingly then, all Category A basins are ancient, dating from the pre-Nectarian. Category B mascons are also old; all 5 are pre-Nectarian. In contrast, the well-preserved types with strong gravitational signatures (Categories C and D) tend to be younger. Only 9 of the 23 are pre-Nectarian, and all 9 are found outside the boundary of the Procellarum Kreep Terrane [*Jolliff et al*., 2000].

[8] Examination of the azimuthally averaged, detrended gravity data for each basin > 300 km in diameter (Figures S1–S41) reveals the nature of the bulls-eye gravity signature. A common characteristic of the central high in both the free-air and Bouguer gravities is that the peak is narrower than the basin itself. Consequently, the negative gravity signal due to the surface depression extends to a larger radius than this central gravity high. Indeed, removal of the topographic component of the gravity from the free-air gravity (yielding the Bouguer gravity) generally eliminates the negative gravity annulus from the Category C basins, implicating the surface topography in the creation of this annulus [cf. *Namiki*

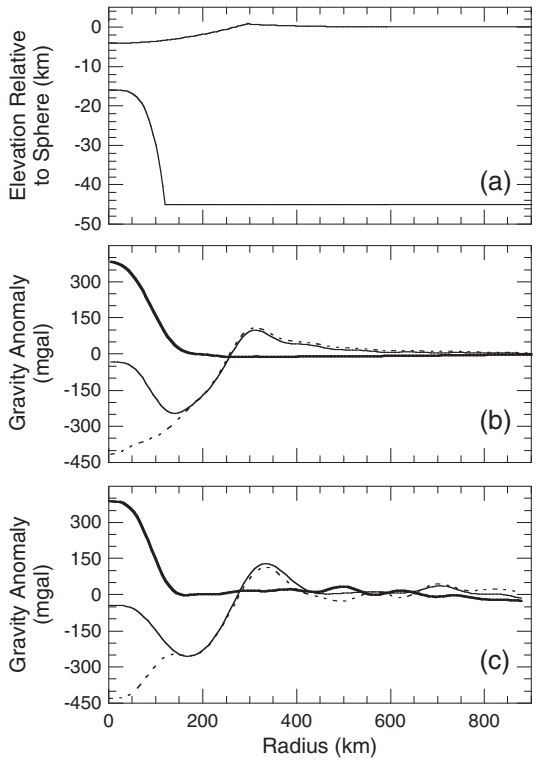

Figure 2. The gravity of a synthetic lunar crater. (a) Profiles of the crustal structure, with a parabolic surface basin with a center-point depth of 4.2 km below datum. At a radius of 295.5 km and elevation of 0.8 km, the basin transitions into an ejecta blanket whose topography falls off as the inverse third power of distance until a radius of 591 km. On the crust-mantle boundary ostensibly 45 km deep, we model topography as an inverted fourth-order polynomial 29 km high and extending to a radius of 120 km (~40% as wide as the surface basin). (b) The free-air (thin solid), topographic (dashed), and Bouguer (thick solid) gravity anomalies from the crustal structure shown in Figure 2a, from a degree-and-order 6–100 spherical harmonic expansion using coefficients calculated using the finite-amplitude method of *Wieczorek and Phillips* [1998]. (c) Radial averaged profiles of the 591 km Category C basin Hertzsprung, for comparison with Figure 2b.

et al., 2009]. Furthermore, the surrounding positive annulus is also absent in the Bouguer gravity, implicating the basin's rim topography.

[9] We can further demonstrate this interplay with a simple basin-like crustal structure. We model the gravity arising from a second-order polynomial basin with a surrounding rim on the surface of a sphere 1737.4 km in radius. On a lunar-like [e.g., *Mohit and Phillips*, 2006] 45 km deep crust-mantle boundary, we model a second-order polynomial as uplifted mantle; this uplifted crust-mantle boundary is narrower than the surface basin. We show this crustal structure in Figure 2a. We then calculate the gravitational potential due to these shapes using the finite-amplitude method of *Wieczorek and Phillips* [1998] and assuming the lunar mass, a crustal density of 2800 kg m^{-3}, and a mantle density of 3300 kg m^{-3}, and then expand the spherical harmonic coefficients from degrees 6–100 (identical to Figures S1–S41). We show these profiles in Figure 2b, along with the gravity profiles from the Category C Hertzsprung basin (Figure 2c); the gravity signatures are very similar. While this exercise does not represent an exhaustive study of the structure beneath Hertzsprung, this example does demonstrate that this simple crustal structure produces the bulls-eye gravity signature of the Category C basins. Thus, it appears that the negative and surrounding positive annuli surrounding mascon basins in the free-air gravity are largely products of the surface topography; *no subsurface mass anomaly is usually required to explain the gravity signal exterior to the central gravity high*.

[10] There are, of course, exceptions to this observation. Some of the smaller mascons show small negative anomalies adjacent to the central peak in the Bouguer gravity; however, these troughs are of a horizontal scale close to the resolution of the spherical harmonic expansion (~110 km full-wavelength for degree 100), and are thus likely just spectral ringing. (GRAIL data will resolve this particular issue.) Some basins still display a regional slope, indicating that a simple truncation of the first 5 spherical harmonic degrees does not remove all regional signals. Only for the largest Category C basin considered (Orientale, as well as Category D Imbrium) is a definitive, localized negative gravity ring surrounding the central high in the Bouguer gravity. This signal is conceivably due to extension of the crust into the mantle associated with deep-seated faulting during the collapse of the transient crater (cf. *Andrews-Hanna and Stewart* [2011]) for these largest basins.

[11] It is interesting to consider the nature of the isostatic state of the basins. An early identifying characteristic of the first discovered mascons [e.g., *Müller and Sjogren*, 1968] was a large, positive free-air gravity anomaly indicating a mass excess that is supported, at least in part, by something other than buoyancy (i.e., superisostasy). Indeed, these basins (our Category D, mare-dominated mascons) still display this characteristic in our analysis. In contrast, the Category C basins display a distinct zoned style of isostasy. The negative and positive free-air annuli indicate subisostatic and superisostatic zones associated with the surface topography. Meanwhile, the central high in the free-air gravity can peak at positive, negative, or near zero (with ~100 mgal of the background). It all depends on whether the subsurface mass excess (as reflected by the Bouguer high) is strong enough to balance or overcome of the negative gravity associated with the low surface topography of the basin's center. Even for those cases where this central free-air peak achieves strongly positive values, it is improper to classify such a basin as superisostatic in its entirety; it is only superisostatic in its central region, surrounded by an annulus that is actually subisostatic (suggesting competing and thereby partially cancelling loads on the lithosphere). Category B basins, on the other hand, tend to be fully isostatic, as demonstrated by the small free-air gravity anomalies at all radii, while the Category A basins are subisostatic, the negligible Bouguer anomalies indicating the free-air gravity largely reflects the remaining surface topography.

3. Discussion

[12] A motivating question of this work is to address why are not all large basins on the Moon mascon basins. Based on the underlying relationship between the age of the basins

and the classification of their gravity signals, we conclude that all >300 km basins are, or at least once were, mascons. Similar to *Mohit and Phillips* [2006], we suggest all large basins start as our Category C, and then evolve into the other types. *Neumann et al*. [1996] and *Wieczorek and Phillips* [1999] showed that with removal of the extensive mare deposits, the crustal structure of Category D basins is similar to Category C. Conversely, *Mohit and Phillips* [2006] explored the conditions that allow either the retention of a mascon or its degradation via viscoelastic relaxation of crust-mantle boundary topography by lower crustal flow. A related analysis, looking at the evolution of the large craters on Mars [*Karimi and Dombard*, 2011], revealed the mechanics. For sufficiently high heat flow coupled with remnant heat from the impact, the brittle-ductile transition occurs within the crust, which results in a mechanical decoupling of the loads from the surface and crust-mantle boundary. The surface load (the basin topography) causes the lithosphere to flex upwards, shallowing the basin, while the subsurface load (the uplifted crust-mantle boundary) flows away via viscous creep, getting progressively lower and wider until gone. If allowed to go to completion, then the end state is a shallowed impact basin, supported by the strength of the lithosphere and overlying a flat crust-mantle boundary. The process often does not go to completion, however, as secular cooling of the planet and dissipation of the impact heat drives the brittle-ductile transition below the crust, halting the evolution. The large basin population on the Moon is consistent with this process. The Category A basins are shallow and have no discernable signal in the Bouguer gravity, indicating near complete relaxation of the uplifted crust-mantle boundary. These basins are all highly degraded and thus ancient, suggesting they date from an early epoch when background heat flows were high enough to permit substantial lower crustal flow. This process appears to have been halted for the Category B basins, which are typically shallower and more degraded than Category C basins, and tend to possess a lower, wider central peak in the Bouguer gravity than Category C basins of comparable diameters (see Supporting Information). Even the Category C basins with central highs that peak at negative values may have experienced some degree of lower crustal flow. The relationship between basin age and the gravity signatures and surface morphologies of large basins points to an evolutionary process that erases mascon signatures and is consistent with studies of the relaxation of basins on the Moon and Mars [*Mohit and Phillips*, 2006, 2007; *Karimi and Dombard*, 2011]. Moreover, it is apparent that this process was considerably more efficient in the pre-Nectarian period than afterward. In addition, no Category C basins exist within the Procellarum Kreep Terrane, a region with thermal properties that may facilitate evolution away from this initial form [cf. *Wieczorek and Phillips*, 1999].

[13] Thus, we can make the reasonable argument that all large lunar basins started with the morphology of a Category C mascon. Because it is only ancient basins that are not mascons, an argument could be made for basin formation being different and not leading to mascons during the pre-Nectarian, presumably an epoch of higher heat flows and thinner lithospheres; however, the existence of the Category B basins, whose morphology is consistent with evolution from a Category C-like initial morphology toward a Category A-like state, argues against this possibility. Thus, the morphology of the Category C mascons hints at their formation. Any uplift of the crust-mantle boundary is driven by the collapse of the transient crater caused by a large isostatic imbalance; however, the transient crater is narrower than the final surface crater, especially for large craters in the gravity-dominated regime. The surface expression of the crater widens and shallows significantly because of inward collapse of the transient crater and adjustment of a large melt sheet [e.g., *Melosh*, 1989; *Spudis*, 1993], a process that apparently does not affect the topography on the crust-mantle boundary. Indeed, hydrocode simulations of large impacts show that the central uplift of the crust-mantle boundary is narrower than the final surface basin [e.g., *Collins et al*., 2002]. In this light, it is not surprising that horizontal scale of the topographies on the surface and crust-mantle boundary differs. The crust-mantle boundary is attempting to achieve isostasy with the transient crater, while the transient crater not only undergoes uplift but also inward collapse.

[14] An important issue is the origin of the mass excess for those Category C basins with a superisostatic central high. Based on the discussion above, one might argue the mass excess is rebounded mantle that overshot the current isostatic balance point during collapse of the transient crater, and then froze with dissipation of the impact shock energy (and subsequent material stiffening). *Kiefer et al*. [2011], however, argued that with the addition of remnant impact heat and its weakening of the lithosphere, any such superisostatic load could not be supported and would collapse toward isostasy. In that case, the superisostatic mass excess would have to arise tens to hundreds of millions of years after the basin's formation and diffusion of the impact heat. To solve this paradox, *Kiefer et al*. [2011] proposed magmatic intrusion of a rock type denser than the crust. To produce a central high in the free-air gravity up to 200 mgal above the background (not above the bottom of the negative annulus, which is due to surface topography), however, requires 5–10 km of this intrusive igneous rock, depending on its density. With mantle uplifted to a state of isostatic balance during basin formation, a several kilometer deep basin means the crust in the central portion is only ~10 km thick (cf. Figure 2a), suggesting an implausible 50–100% replacement of the basin's central crust with this intrusive rock. This magmatism need not be all intrusive, however; extrusive flows 1–2 km thick, confined within the central peak ring, and fully supported by the strength of the lithosphere can yield this gravity anomaly. Indeed, all 8 of the Category C basins with a superisostatic central gravity high show readily apparent mare volcanism within their peak rings, while the remaining C basins do not. In contrast, *Melosh et al*. [2012] argued for evolution in the density of the rocks, in their case solidification and cooling of the impact melt sheet. A byproduct of their simple simulations, however, was that the negative free-air annulus arises from flexural drawdown of the crust into the mantle; such a state should produce a negative annulus in the Bouguer gravity as well, in contrast with the observed Bouguer gravity.

[15] Again, nothing indicates that all large craters on the Moon did not at least start as mascon basins. Collapse of a sufficiently large transient crater into a low-density crust should yield a mascon basin, but such gravity signatures are uncommon on the other terrestrial planets. Notably while

Isidis is generally agreed to be a mascon, the nature of the other large basins is equivocal [e.g., *Yuan et al*., 2001; *Arkani-Hamed*, 2009]. Curiously, Mars has no mascons in the size range we consider here for the Moon. *Mohit and Phillips* [2007] and *Karimi et al*. [2012] have demonstrated, however, that for Martian basins 200–1000 km in diameter, the lack of significant crust-mantle boundary uplift is consistent with lower crustal flow of initially much larger uplift; indeed, the predicted heat flows track the expected secular cooling of the planet as well as mark a spatial pattern associated with the crustal dichotomy. An initial search for mascon basins on Mercury was not definitive due to the resolution of the gravity field [*Smith et al*., 2012]; the Caloris Basin is the only one with a definitive positive free-air gravity anomaly, although it may be at least partially attributed to high topography on the basin floor. On Venus, only Mead Crater (~270 km in diameter) is large enough to be (barely) resolved in Magellan gravity models. Analysis suggests a subisostatic crater with negligible uplift of the crust-mantle boundary [*Banerdt et al*., 1994], but with its thick crust, high surface temperature, and near-Earth-like heat flow, lower crustal flow might be fairly efficient on Venus [cf. *Dombard et al*., 2007]. Earth definitely has Earth-like heat flow; however, large craters are uncommon and highly degraded, rendering a companion analysis difficult.

4. Conclusions

[16] The gravitational signature of a large basin on a terrestrial planet should be that of a bulls-eye, with a large central positive surrounded by annuli of negative then positive free-air gravity, a by-product of the formation of the basin. Upward and inward collapse of the transient crater and adjustment of the melt sheet yields a surface basin wider than the initial transient crater, yet uplift of the crust-mantle boundary appears to respond to a large isostatic imbalance with the transient crater. Thus, the uplifted mantle will be narrower than the surface depression. This structure yields a bulls-eye gravity pattern: the excess gravity from the uplifted mantle is too narrow to overcome the negative gravity of the surface topography near but inward of the crater rim. The positive gravity annulus exterior to the basin reflects the rim topography. These basins are thus not super- or subisostatic, but have zoned states of isostasy. The loads arising from these differing isostasy zones will partially cancel, explaining some of the lithospheric support of mascon loads. Large basins that are not mascons or with differing gravitational characteristics likely began as mascon basins with this bulls-eye gravity pattern; extensive mare fill or lower crustal flow can lead to the evolution away from this initial type. Thus, formation of mascon basins may be common on the Moon and other terrestrial planets.

[17] **Acknowledgments.** This work was supported by NASA grant NNX08AZ03G to SAH. We thank D. Nunes and S. Smrekar for reviews that helped sharpen the manuscript.

References

Andrews-Hanna, J. C., and S. T. Stewart (2011), The crustal structure of Orientale and implications for basin formation, Abstract 2194, paper presented at Lunar and Planet. Sci. Conf. XLII, Lunar and Planet. Inst., Houston.

Arkani-Hamed, J. (2009), Polar wander of Mars: Evidence from giant impact basins, *Icarus*, *204*, 489-498.

Banerdt, W. B., A. S. Konopliv, N. J. Rappaport, W. L. Sjogren, R. E. Grimm, and P. G. Ford (1994), The isostatic state of Mead Crater, *Icarus*, *112*, 117-129.

Collins, G. S., H. J. Melosh, J. V. Morgan, and M. R. Warner (2002), Hydrocode simulations of Chicxulub Crater collapse and peak-ring formation, *Icarus*, *157*, 24-33.

Dombard, A. J., C. L. Johnson, M. A. Richards, and S. C. Solomon (2007), A magmatic loading model for coronae on Venus, *J. Geophys. Res.*, *112*, E04006, doi:10.1029/2006JE002731.

Jolliff, B. L., J. J. Gillis, L. A. Haskin, R. L. Korotev, and M. A. Wieczorek (2000), Major lunar crustal terranes: Surface expressions and crust-mantle origins, *J. Geophys. Res.*, *105*, 4197-4216.

Karimi, M., and A. J. Dombard (2011), The evolution of subsurface and surface topography of large craters on Mars, Abstract P43D-1712 presented at 2011 Fall Meet., AGU, San Francisco, CA, 5-9 Dec.

Karimi, M., A. J. Dombard, and R. M. Williams (2012), A study of the thermal evolution of Mars via viscoelastic relaxation of large craters, Abstract 2712, paper presented at Lunar and Planet. Sci. Conf. XLIII, Lunar and Planet. Inst., Houston

Kiefer, W. S., P. J. McGovern, R. W. Potter, G. S. Collins, and D. A. Kring (2011), The collapse of super-isostacy: Volcanic intrusions as an alternative model for lunar mascon gravity anomalies, Abstract P33G-02 presented at 2011 Fall Meet., AGU, San Francisco, CA, 5-9 Dec.

Melosh, H. J. (1989), Impact Cratering, a Geologic Process, Oxford Univ. Press, Oxford.

Melosh, H. J., D. M. Blair, and A. M. Freed (2012), Origin of superisostatic gravity anomalies in lunar basins, Abstract 2596, paper presented at Lunar and Planet. Sci. Conf. XLIII, Lunar and Planet. Inst., Houston.

Mohit, P. S., and R. J. Phillips (2006), Viscoelastic evolution of lunar multiring basins, *J. Geophys. Res.*, *111*, E12001, doi:10.1029/2005JE002654.

Mohit, P. S., and R. J. Phillips (2007), Viscous relaxation on early Mars: A study of ancient impact basins, *Geophys. Res. Lett.*, *34*, L21204, doi:10.1029/2007GL031252.

Müller, P. M., and W. L. Sjogren (1968), Mascons: Lunar mass concentrations, *Science*, *161*, 680-684.

Namiki, N., et al. (2009), Farside gravity field of the Moon from four-way Doppler measurements of SELENE (Kaguya), *Science*, *323*, 900-905.

Neumann, G. A., M. T. Zuber, D. E. Smith, and F. G. Lemoine (1996), The lunar crust: Global structure and signature of major basins, *J. Geophys. Res.*, *101*, 16841-16864.

Phillips, R. J., J. E. Conel, E. A. Abbott, W. L. Sjogren, and J. B. Morton (1972), Mascons: Progress toward a unique solution for mass distribution, *J. Geophys. Res.*, *77*, 7106-7114.

Smith, D. E., et al. (2012), Gravity field and internal structure of Mercury from MESSENGER, *Science*, *336*, 214-217.

Spudis, P. D. (1993), The Geology of Multi-ring Impact Basins: The Moon and Other Planets, Cambridge Univ. Press, Cambridge.

Wieczorek, M. A., and R. J. Phillips (1998), Potential anomalies on a sphere: Application to the thickness of the lunar crust, *J. Geophys. Res.*, *103*, 1715-1724.

Wieczorek, M. A., and R. J. Phillips (1999), Lunar multiring basins and the cratering process, *Icarus*, *139*, 246-259.

Wise, D. U., and M. T. Yates (1970), Mascons as structural relief on a lunar Moho, *J. Geophys. Res.*, *75*, 261-268.

Yuan, D.-N., W. L. Sjogren, A. S. Konopliv, and A. B. Kucinskas (2001), Gravity field of Mars: A 75th degree and order model, *J. Geophys. Res.*, *106*, 23377-23401.

Zuber, M. T., et al. (2012), Preliminary results on the structure of lunar highland crust from GRAIL gravity and LOLA altimetry, Abstract 9015, paper presented at Second Conf. on Lunar Highlands Crust, Lunar and Planet. Inst. Bozeman, MT.